TOPOLOGY OPTIMIZATION OF COUPLING BETWEEN SLAB AND PHOTONIC CRYSTAL WAVEGUIDE

Koichi Hirayama[1], Yoshihiro Tabata[1], Yasuhide Tsuji[1], and Yukinari Hayashi[1]

[1] Kitami Institute of Technology, 165 Koen-cho, Kitami, 090-8507, Japan

Corresponding author: Prof. Koichi Hirayama
Email: hirakc@mail.kitami-it.ac.jp
Tel: +81-157-26-9285
Fax: +81-157-25-1087

ABSTRACT:
We employ topology optimization with the finite-element method to improve the coupling between a slab waveguide and a photonic crystal waveguide. Here, we apply topology optimization in a small design region to realize the improvement of the coupling. Also, we simplify an optimized structure of the coupling region for easier fabrication and try to find core features of the optimized structure.

Key words:
topology optimization; finite-element method; photonic crystal waveguide; waveguide junction

1. INTRODUCTION

Optical waveguide devices of compact size and high performance have been developed with the advance of recent optical communication system. Structures of optical waveguide devices are usually designed based on the improvement of conventional devices or on heuristic idea. Recently, the design of optical waveguide devices based on optimization methods has also been reported, which is enabled by the advent of low-cost and high-powered computers.

In the field of structure analysis, in addition to sizing and shape optimization, topology optimization [1] has been advanced, and recently it is applied to some optimization problems in the field of electromagnetic wave. In sizing and shape optimization, the location and shape of blocks of material in a design region are designed to maximize or minimize a specific objective function, while topology in a design region, such as the number and connectivity of blocks of material, remains fixed. Topology optimization involves the determination of features in a design region, such as the location, shape, number and connectivity of blocks of material, so that we could expect to obtain a novel configuration using topology optimization. In photonic crystal waveguides, the optimization of a bend [2-6] and the improvement of radiation characteristic into free space [7] have been investigated. Also, 90-degree bend of an optical waveguide [8] has been reported.

In this paper, we employ topology optimization with the finite-element method (FEM) to improve the coupling between a slab waveguide and a photonic crystal (PhC) waveguide. A similar work has been done in [9], but it focuses on slow light regime and a relatively large design region of the optimization is needed. Here, we apply topology optimization in a small design region to realize the improvement of the coupling. Also, we simplify an optimized structure of the coupling region for easier fabrication and try to find core features of the optimized structure.

2. FINITE ELEMENT ANALYSIS OF COUPLING BETWEEN SLAB AND PhC WAVEGUIDE

We consider the coupling between a slab waveguide and a PhC waveguide, as shown in Figure 1, where boundaries Γ_1 and Γ_2 are the input and output ports, respectively, and we assume the field has no variation in the z direction. Symbol a represents the lattice constant of the triangular lattice of the PhC, and r is the radius of air hole of the PhC. Symbol d is the thickness of the slab waveguide, and ε_0 and $\varepsilon_0\varepsilon_{rd}$ are permittivities of air and dielectric, respectively. Dividing analysis region Ω, including PML, into a number of triangular quadratic elements and applying the FEM, we obtain

a final matrix equation as follows:

$$[P]\{\phi\} = \{Q\} \qquad (1)$$

where $[P]$ is a matrix generated by the FEM, $\{Q\}$ is a vector related to an incident wave, $\phi = H_z$ or E_z (H_z and E_z being the z component of magnetic and electric field, respectively) for TE or TM mode, which is characterized by the lack of the z component of electric or magnetic field, respectively. After solving Eq. (1), we can compute the S parameter in waveguide n for the incidence of a propagating mode with unit amplitude from waveguide 1 as follows:

$$S_{n1} = -\delta_{n1} + \{g_n\}^T \{\phi_n\} \qquad (2)$$

where δ_{n1} represents the Kronecker delta, $\{g_n\}$ is a known vector related to a propagating mode in waveguide n, $\{\phi_n\}$ is a vector which has the values of ϕ on boundary Γ_n, and superscript T denotes a transpose.

3. TOPOLOGY OPTIMIZATION AND SENSITIVITY ANALYSIS

Topology optimization determines material distribution in a design region through the optimization procedure. To find the distribution of dielectric with relative permittivity ε_{rd} in air, we employ the following expression for the material distribution of the i-th triangular element in a design region:

$$\varepsilon_{ri} = 1 + (\varepsilon_{rd} - 1)\rho_i^p, \quad 0 \le \rho_i \le 1 \qquad (3)$$

where ρ_i is referred to as density, and p is a constant usually greater than two and $p = 3$ in this paper.

Let C be an objective function, which is minimized or maximized in an optimization problem. To employ the method of moving asymptotes (MMA) [10] to optimize density ρ_i, we should find the derivative of the objective function with respect to the density of a triangular element, $\partial C / \partial \rho_i$, referred to as sensitivity. Since a design region is composed of a large number of triangular elements, it is very time-consuming to compute each of the derivatives with a difference approximation technique. To avoid it, we employ the adjoint variable method (AVM) [1]. In most cases of waveguide problems, C is explicitly expressed with the absolute values of S parameters, and its sensitivity is calculated as follows:

$$\frac{\partial C}{\partial \rho_i} = \sum_{n=1}^{2} \frac{\partial C}{\partial |S_{n1}|} \mathrm{Re}\left(\frac{S_{n1}^*}{|S_{n1}|} \frac{\partial S_{n1}}{\partial \rho_i} \right) \qquad (4)$$

where Re stands for the real part of a complex number and superscript * indicates complex conjugate. From Eqs. (1) and (2), we obtain

$$\frac{\partial [P]}{\partial \rho_i}\{\phi\} + [P]\frac{\partial \{\phi\}}{\partial \rho_i} = \{0\}, \quad \frac{\partial S_{n1}}{\partial \rho_i} = \{\tilde{g}_n\}^T \frac{\partial \{\phi\}}{\partial \rho_i} \tag{5}$$

where $\{\tilde{g}_n\}$ is a vector whose components are the values of $\{g_n\}$ at the nodes on boundary Γ_n and zero elsewhere, and $\{0\}$ is a null vector. Using Eqs. (4) and (5), we can derive the following expression for the sensitivity:

$$\frac{\partial C}{\partial \rho_i} = \sum_{n=1}^{2} \frac{\partial C}{\partial |S_{n1}|} \mathrm{Re}\left[\frac{S_{n1}^*}{|S_{n1}|} \{\Phi_n\}^T \left(-\frac{\partial [P]}{\partial \rho_i}\{\phi\} \right) \right], \quad \{\Phi_n\} = ([P]^T)^{-1}\{\tilde{g}_n\} \tag{6}$$

4. NUMERICAL RESULTS

In Figure 1, the relative permittivity of dielectric is $\varepsilon_{rd} = 5.1074$, which corresponds to an effective relative permittivity for an air-bridged dielectric with thickness of $0.32a$ and relative permittivity of 10 at $a/\lambda = 0.334$ (λ being the wavelength in vacuum). The photonic bandgap for TE wave is computed as $a/\lambda = 0.312$ to 0.366 using the FEM for the two-dimensional periodic structure. The fundamental TE mode of a slab waveguide with the thickness of $d = \sqrt{3}a - 2r$ is incident from boundary Γ_1, and the transmission is evaluated at boundary Γ_2. PML is employed to prevent non-desired reflection. Two rectangles of the input and output side in the PhC waveguide, drawn in broken line in Figure 1, represent design regions for optimization. Here, we optimize the design regions to maximize the normalized transmission power, $|S_{21}|^2$, in the bandwidth of $a/\lambda = 0.325$ to 0.350.

First, we investigate the dependence of an optimized structure on an initial structure in the design region. Figure 2 shows optimized structures of the input side for three pairs of initial densities at air hole and dielectric in the unoptimized structure, i.e., (ρ_a, ρ_d)=(0.1,0.9), (0.3,0.7), (0.5,0.5), where green and red areas represent air and dielectric, respectively, while the areas shown in other colors represent material with intermediate relative permittivity between air and dielectric. For comparison, we show an optimized structure for a design region which is half as large as that in Figure 1 and has the initial density of (ρ_a, ρ_d)=(0.1,0.9). In these cases, the optimized structure of the output side is the same as that of the input side, although it is not a constraint condition in optimization. Moreover, we performed the optimization for more three pairs of initial densities, and we confirmed that optimized structures for

(ρ_a, ρ_d) =(0,1),(0.2,0.8) are almost the same as that at (ρ_a, ρ_d) =(0.1,0.9), and an optimized structure for (ρ_a, ρ_d) =(0.4,0.6) is almost the same as that at (ρ_a, ρ_d) =(0.5,0.5). Figure 3 shows the normalized transmission power versus the normalized frequency for the optimized structures in Figure 1. We find that the optimized structures at (ρ_a, ρ_d) =(0.1,0.9), (0.3,0.7) are preferred because of easy fabrication and excellent transmission characteristic. Also, we observe that half size of the design region is too small to obtain good transmission characteristic.

Finally, we simplify the optimized structure of the coupling region at (ρ_a, ρ_d) =(0.1,0.9) for easier fabrication and try to find core features of the obtained optimized structure. Figure 4 shows four simplified structures for the optimized structure, where structures 1 to 4 are the structures simplified in order of number. Also, Figure 5 shows the reflection and transmission characteristics of the simplified structures and the unoptimized one, and we notice that the simplified structure have better transmission characteristic than that of the unoptimized one. Moreover, the normalized transmission power of structures 1 to 3 is almost more than 90 percent in the bandwidth of $a/\lambda = 0.325$ to 0.350 for the optimization, but structure 4 is not so. Structures 1 to 4 have a common geometry that the waveguide width is broadened from d to $d+2r$ in the connection of the slab waveguide to the PhC one, and we notice that the geometry plays a primary role in the modification of the transmission characteristic. Also, structure 4 does not have a triangular projection between the slab waveguide and the PhC one, unlike structures 1 to 3, so that we find that the projection is necessary for obtaining better transmission characteristic.

5. CONCLUSION

We applied topology optimization with the FEM to improve the coupling between a slab waveguide and a photonic crystal waveguide, and obtained an optimized structure with excellent transmission characteristic in a small design region for the coupling. Also, we simplified the optimized structure of the coupling region for easier fabrication, and were able to find some core features of the optimized structure.

ACKNOWLEDGEMENTS

The authors thank Prof. K. Svanberg for his computer codes of MMA.

Figure Captions

Figure 1: Geometry of coupling between a slab waveguide and a PhC waveguide

Figure 2: Optimized structure for some initial densities (ρ_a, ρ_d), where ρ_a and ρ_d represent initial densities at air hole and dielectric in the unoptimized structure, respectively, and `half' means that the design region is half size of that in Figure 1

Figure 3: Transmission characteristic for the optimized structures shown in Figure 2

Figure 4: Simplified structures for the optimized structure at $(\rho_a, \rho_d) = (0.1, 0.9)$

Figure 5: Reflection and transmission characteristics of the simplified structures shown in Figure 4

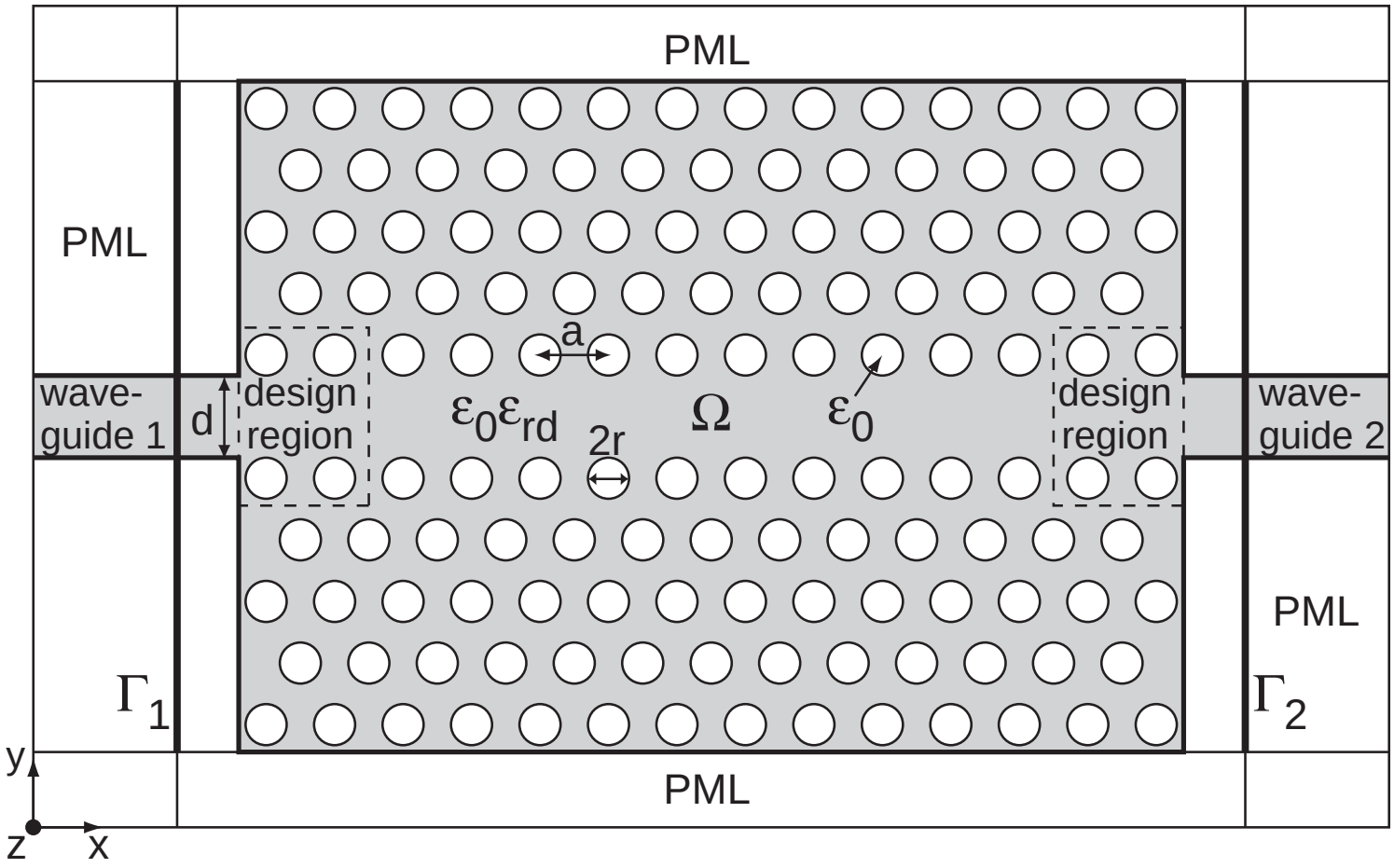
PML
PML
wave-
guide 1
d
design
region
a
$\varepsilon_0\varepsilon_{rd}$
2r
Ω
ε_0
design
region
wave-
guide 2
PML
Γ_1
Γ_2
PML
y
z
x

Figure 1

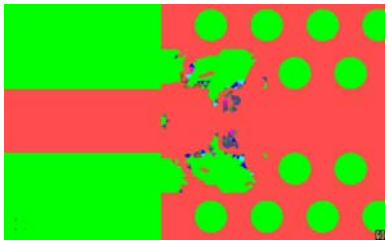

$(\rho_a,\rho_d)=(0.1,0.9)$

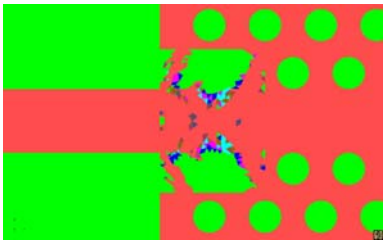

$(\rho_a,\rho_d)=(0.3,0.7)$

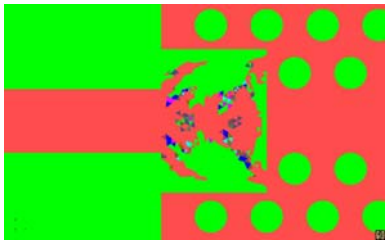

$(\rho_a,\rho_d)=(0.5,0.5)$

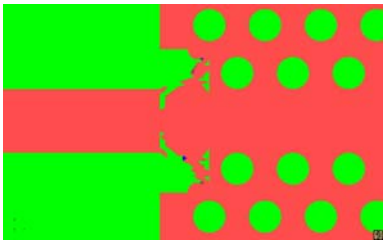

$(\rho_a,\rho_d)=(0.1,0.9)$, half

Figure 2

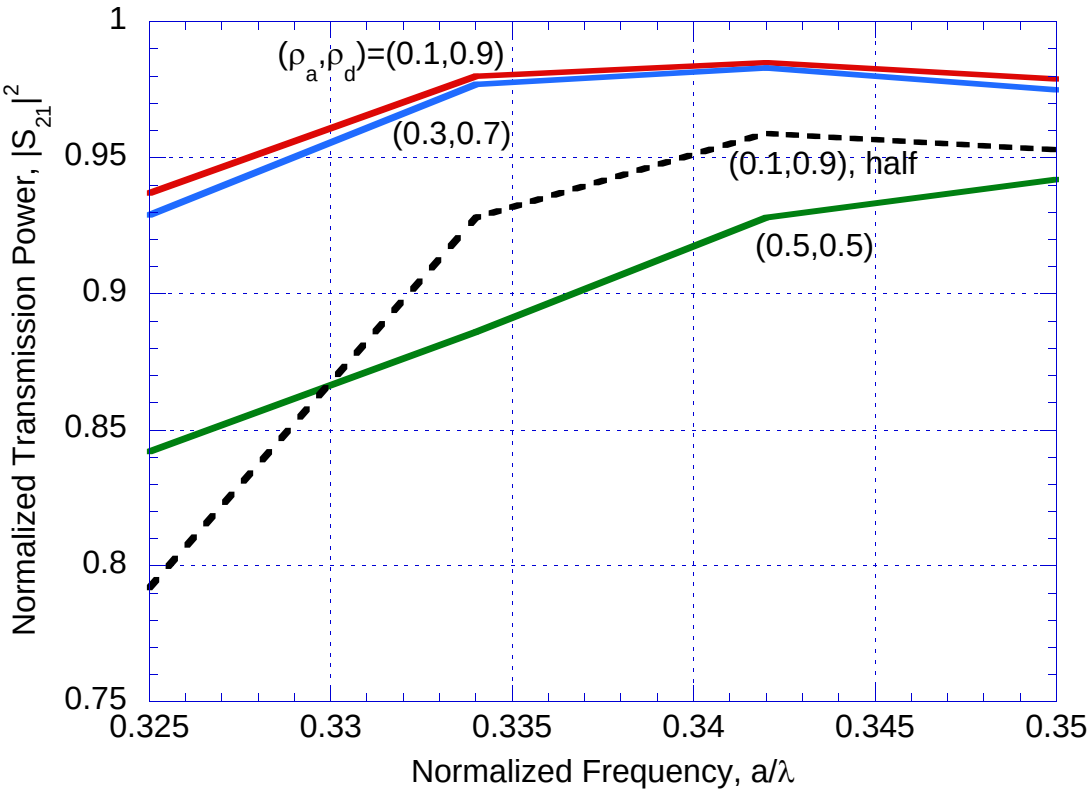
1
0.95
0.9
0.85
0.8
0.75
0.325
0.33
0.335
0.34
0.345
0.35
Normalized Transmission Power, |S21|2
Normalized Frequency, a/λ
(ρa,ρd)=(0.1,0.9)
(0.3,0.7)
(0.1,0.9), half
(0.5,0.5)

Figure 3

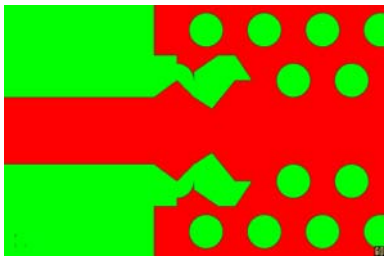

Structure 1

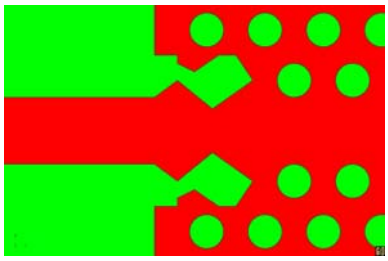

Structure 2

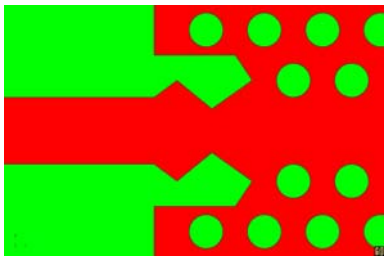

Structure 3

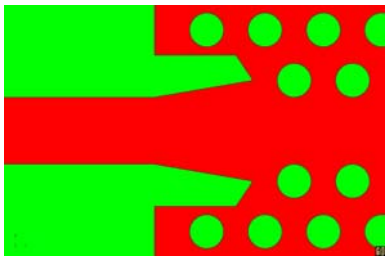

Structure 4

Figure 4

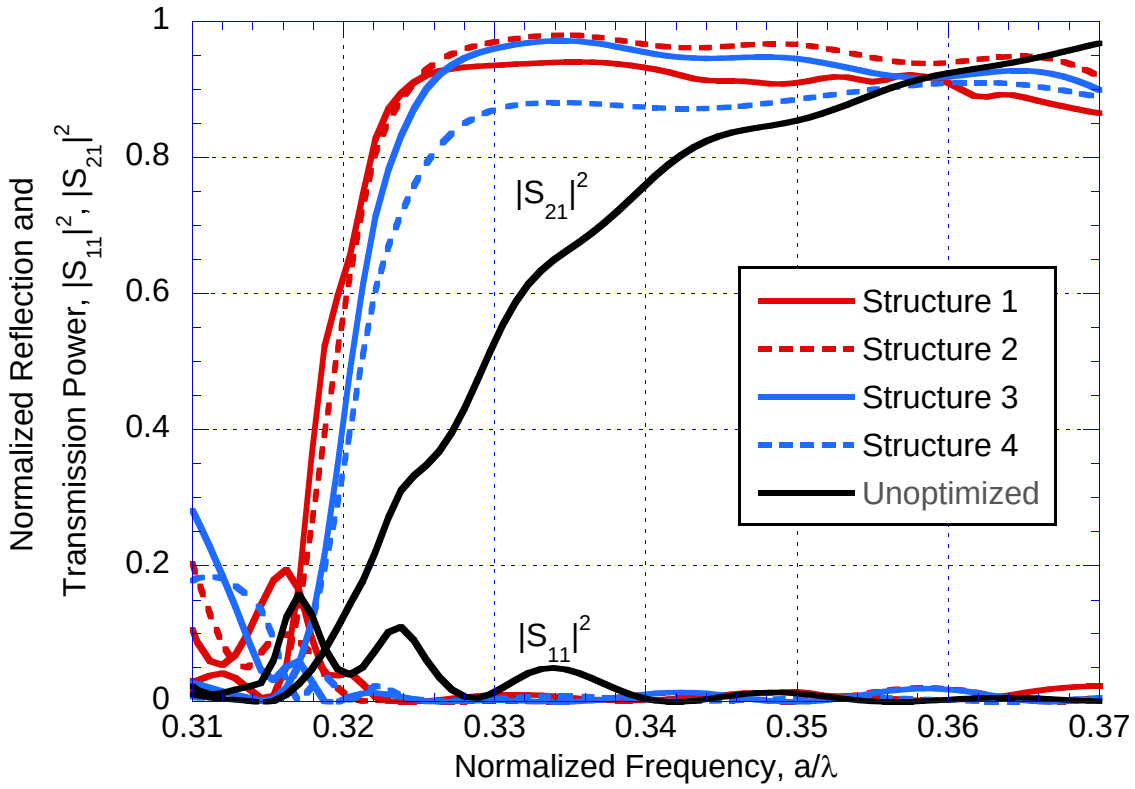
Normalized Reflection and
Transmission Power, $|S_{11}|^2$, $|S_{21}|^2$
1
0.8
0.6
0.4
0.2
0
0.31
0.32
0.33
0.34
0.35
0.36
0.37
Normalized Frequency, a/λ
$|S_{21}|^2$
$|S_{11}|^2$
Structure 1
Structure 2
Structure 3
Structure 4
Unoptimized

Figure 5